

LETTER • OPEN ACCESS

Estimating the impact of shelterbelt structure on corn yield at a large scale using Google Earth and Sentinel 2 data

To cite this article: Yage Liu *et al* 2022 *Environ. Res. Lett.* 17 044060

View the [article online](#) for updates and enhancements.

You may also like

- [Assessing the effectiveness and pathways of planned shelters in protecting mental health of flood victims in China](#)
Shuang Zhong, Minghui Pang, Hung Chak Ho *et al.*
- [Impacts of varying agricultural intensification on crop yield and groundwater resources: comparison of the North China Plain and US High Plains](#)
Hongwei Pei, Bridget R Scanlon, Yanjun Shen *et al.*
- [Declining Potential Yield and Rain-fed Yield of Corn in the Corn Belt of Northeastern China during the Past Three Decades](#)
Zhe Pang and Zenghui Sun

ENVIRONMENTAL RESEARCH
LETTERS

LETTER

Estimating the impact of shelterbelt structure on corn yield at a large scale using Google Earth and Sentinel 2 data

OPEN ACCESS

RECEIVED

5 December 2021

REVISED

21 February 2022

ACCEPTED FOR PUBLICATION

25 February 2022

PUBLISHED

4 April 2022

Original content from this work may be used under the terms of the [Creative Commons Attribution 4.0 licence](#).

Any further distribution of this work must maintain attribution to the author(s) and the title of the work, journal citation and DOI.

Yage Liu^{1,2} , Huidong Li^{1,*}, Fenghui Yuan^{1,3} , Lidu Shen¹, Minchao Wu⁴ , Wenliang Li⁵, Anzhi Wang¹, Jiabing Wu¹ and Dexin Guan¹¹ CAS Key Laboratory of Forest Ecology and Management, Institute of Applied Ecology, Chinese Academy of Sciences, Shenyang, People's Republic of China² College of Resources and Environment, University of Chinese Academy of Sciences, Beijing, People's Republic of China³ Department of Soil, Water, and Climate, University of Minnesota, Saint Paul, MN United States of America⁴ Department of Earth Sciences, Uppsala University, Uppsala, Sweden⁵ Department of Geography, Environment, and Sustainability, University of North Carolina at Greensboro, Greensboro, United States of America

* Author to whom any correspondence should be addressed.

E-mail: huidong.li@iae.ac.cn**Keywords:** shelterbelt structure, windbreak width-gap grade, maize yield profile, yield increase effect, windbreak density, Sentinel 2, Google EarthSupplementary material for this article is available [online](#)**Abstract**

A shelterbelt is an important measure to protect farmland and increase crop yield. However, how a shelterbelt structure affects crop yield is still unclear due to the difficulties accessing sufficient data from traditional field observations. To address this problem, we developed an innovative framework to estimate the shelterbelt structure and crop yield profile at a regional scale based on Google Earth and Sentinel-2 data. Using this method, we quantified the impact of the shelterbelt structure on the corn yield at 302 shelterbelts in the Northeast Plain of China. Generally, the corn yield increased (by 2.41% on average) within a distance of 1.2–15 times the tree height from the shelterbelt. Such an effect was particularly prominent within a distance of two to five times the tree height, where the corn yield was significantly increased by up to 4.63%. The structure of the shelterbelt has a significant effect on the magnitude of increase in yield of the surrounding corn. The increment of corn yields with high-, medium-high-, medium- and low-width-gap grade shelterbelt were 2.01%, 2.21%, 1.99%, and 0.91%, respectively. The medium-high grade shelterbelt achieved the largest yield increase effect. The location of the farmland relative to the shelterbelt also affected the yield, with a yield increase of 2.39% on the leeward side and 1.89% on the windward side, but it did not change the relationship between the yield increase effect and the shelterbelt structure. Our findings highlight the optimal shelterbelt structure for increasing corn yield, providing practical guidance on the design and management of farmland shelterbelts for maximizing yield.

1. Introduction

A farmland shelterbelt, a strip corridor dominated by trees, plays an important role in the sustainable development of an agroforestry ecosystem. A shelterbelt can efficiently benefit the growth of surrounding crops (Kort 1988, Baker *et al* 2018, Smith *et al* 2021) by reducing soil erosion (Haddaway *et al* 2018, Fang 2021, Su *et al* 2021) and wind disasters (Cleugh *et al* 1998, Guan *et al* 2003, Yuan *et al* 2020) and

improving the microclimate for crop growth (Kanzler *et al* 2019, Baker *et al* 2021). Moreover, the presence of a shelterbelt creates more habitats for birds and bees, reduces the occurrence of pests and diseases, and reduces pesticide drift, thereby indirectly increasing crop yield (Bentrup *et al* 2019, Gochez *et al* 2020, Weninger *et al* 2021). Previous studies reported that a shelterbelt could increase the corn yield, by 4%–9% (Zheng *et al* 2016) on average, and by up to 56% in some cases (Kort 1988, Rivest and Vezina 2015,

Osorio *et al* 2019). Therefore, the construction of shelterbelts is vital to protect farmland and secure food supply.

The impact of a shelterbelt on crop yield is significantly affected by its structure, such as height, orientation, and density (Patil *et al* 2002, Amichev *et al* 2017, Hansen *et al* 2020, Zhu and Song 2021). The yield increase effect was found to be proportional to tree height and most significant within the distance of 20 H (H: tree height) (Kort 1988, Kenney 1992, Smith *et al* 2021). The orientation of the shelterbelt largely changed wind speed and subsequently affected crop yield (Tamang *et al* 2010). Shelterbelts perpendicular to the prevailing wind were the most effective layout in increasing crop yield (Zhu *et al* 2003). The density of the shelterbelt was another influencing factor of shelter efficiency. Previous studies found that the difference in the yield increase effect caused by shelterbelt density could exceed 10% (Jiang *et al* 2003). Wu *et al* (2018) and Iwasaki *et al* (2021) proposed a suspicion of the optimal shelterbelt density to maximize the protection efficiency. Shelterbelt density was traditionally expressed by porosity, which is a 2D indicator defined as the percentage of open space in the windbreak to its total volume (Zhou *et al* 2002, Guan *et al* 2009, Wu *et al* 2018). But recent research found that 3D indicators more accurately describe shelterbelt density, such as shelterbelt width, total area density and gap fraction (Deng *et al* 2013, Iwasaki *et al* 2020). However, these parameters were difficult to obtain at a large scale based on field observations (Yang *et al* 2017). In addition, previous studies on shelterbelt structure mainly focused on its impact on the farmland environment but rarely focused on its crop yield effect (Wu *et al* 2018, Liu *et al* 2021). Thus, it is necessary to conduct large-scale studies to investigate the relationship between shelterbelt structure and crop yield.

The impact of a shelterbelt on crop yield is usually investigated using yield profiles (i.e. the crop yield versus the distance from the shelterbelt). The yield profile around the shelterbelt usually consists of two sections: yield-reduced section near the shelterbelt and yield-increased section far from the shelterbelt (Helmert and Brandle 2005, Osorio *et al* 2019). The reduced crop yield near the shelterbelt is caused by the competition between trees and crops, whereas the increased crop yield in the far areas is induced by the protective effect of the shelterbelt. Most studies obtained the yield profile through field measurements (Kort 1988, Sudmeyer *et al* 2002, Ding and Su 2010, Rivest and Vezina 2015). Although this method can accurately assess the shelterbelt's impact on crop yield, it is laborious, time-consuming, and can only be operated on a small scale. Therefore, previous studies about the impact of shelterbelts on crop yield were usually restricted to a few shelterbelts and the impacts of different shelterbelt structures were ignored (Bao *et al* 2012, Rivest and Vezina 2015, Swieter *et al* 2019,

Weninger *et al* 2021). Remote sensing measurement can access shelterbelts and crop yield information at a large scale. Recent studies have successfully used remote sensing data to explore the impact of shelterbelts on crop yield (Zheng *et al* 2016, Iwasaki *et al* 2019, Li *et al* 2020). However, due to the lack of reliable methods and fine resolution remote sensing data, detecting shelterbelts and measuring their structure and crop yield profile at a large scale is still challenging.

In this study, we developed an innovative framework to estimate shelterbelt structure and corn yield profile using state-of-the-art high-resolution remote sensing data. Specifically, the Google earth data were used to extract shelterbelt information for the measuring of shelterbelt structures at a regional scale. High-resolution Sentinel-2 data were used to calculate corn yield profiles. Using this method, we investigated 302 shelterbelts in Northeast China and first quantified the impact of shelterbelt width and gap fraction grade on corn yield. The underlying mechanisms of corn yield change under different shelterbelt structures were discussed. Our findings can help us better understand shelterbelt impacts on crop yield and to guide the practical management of shelterbelts based on their structure to improve corn yield.

2. Study area, data, and method

2.1. Study area

The study area is located on the Songliao Plain in Northeast China, which is the largest farmland shelterbelt district (54 260 km²) and one of the essential grain-producing areas in China (figure 1). The study area is included in the Three-North Shelter Forest Program, which is the largest ecological afforestation program worldwide (Yu *et al* 2006). The shelterbelts have been well planned, constructed, and managed by the professional agency since 1978 (Zhang *et al* 2017). Poplar is the dominant tree species (mainly include *Populus simonii*, *Populus × xiaozhuanica*, *Populus pseudo-simonii* and *Populus × beijingensis*), accounting for more than 98% of all farmland shelterbelt planting areas (Zhu and Zheng 2019). The major crop within the sheltered farmland is corn (*Zea mays* L.), growing from mid-April to late September. The region is at the junction of semi-humid and semi-arid regions with continental and monsoon climate characteristics. The mean air annual temperature is 1 °C–7 °C, the mean annual precipitation is 300–550 mm (Zheng *et al* 2016). According to the statistics of the daily average wind data from 1981 to 2015 at six national weather stations in the study area (triangle in figure 1), the average wind speed during the growing season was 2.5–3.3 m s⁻¹, and the dominant wind direction of all stations is south-southwest (figure 1). The maximum and minimum wind speed occurred in May and August, respectively.

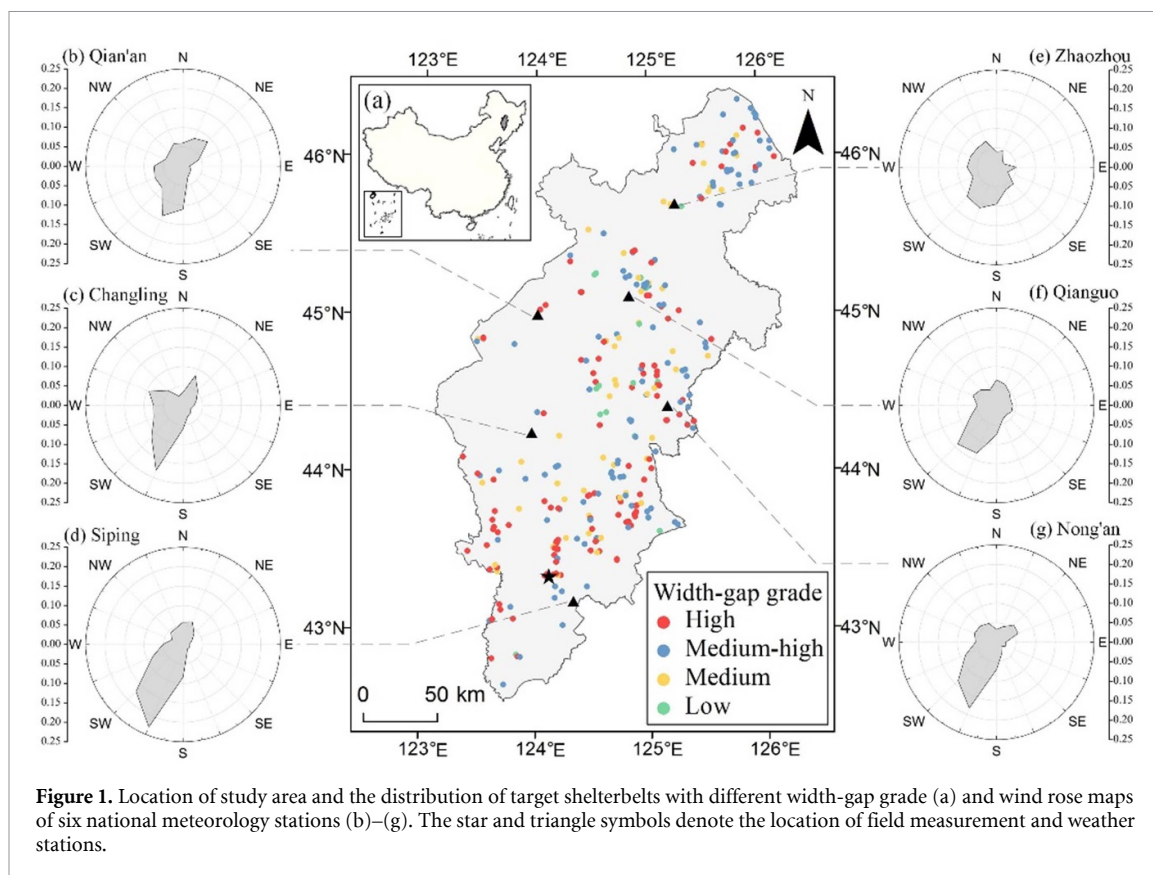


Figure 1. Location of study area and the distribution of target shelterbelts with different width-gap grade (a) and wind rose maps of six national meteorology stations (b)–(g). The star and triangle symbols denote the location of field measurement and weather stations.

2.2. Data procedures

2.2.1. Google Earth data

Google Earth data were used to identify the target shelterbelts and measure their geometric parameters (i.e. shelterbelt width, shelterbelt length, gap length, farmland length, and corn row-shelterbelt angle) (figure 2(a)). Google Earth® provides sub-meter spatial resolution geospatial datasets with red-green-blue bands worldwide (Liang *et al* 2018) and has been widely applied for geometric measurements (Ding *et al* 2020). The Google Earth images from 2016 to 2019 were obtained from Google Earth Pro software (www.google.com/earth/versions/#earth-pro).

2.2.2. Sentinel-2 data

Sentinel-2 data were used to calculate leaf area index (LAI) and subsequently estimate corn yield. Sentinel-2 is a constellation of two satellites in the same orbit operated by the European Space Agency, with a spatial resolution of 10–60 m and a temporal resolution of about five days in the study area (Drusch *et al* 2012). Sentinel-2 data has been widely used in yield estimation, growth monitoring, and crop type identification (Clevers *et al* 2017, Kayad *et al* 2019). The previous studies of Gao *et al* (2018), Lambert *et al* (2018), and Skakun *et al* (2021) found the time window of 30–60 d before harvest (late July to early September) was the optimal period for corn yield estimation using Sentinel-2 data, as this period corresponds to

the reproductive stage in phenological development with the largest LAI. Accordingly, we used Sentinel-2 data in this time window to calculate the corn LAI and yield. Sentinel-2 data from 2016 to 2019 were acquired from <https://scihub.copernicus.eu/> and processed in Sentinel Application Platform (SNAP) software (<http://step.esa.int/main/>). The data of all used bands (resolutions from 10 to 60 m) were resampled to 10 m.

2.2.3. Field measurement of corn yield

We used field measurement of corn yield data to estimate and validate the parameters of the corn yield profile model. The field measurements (figure 1) were conducted in the Conservation Tillage Research and Development Station of the Chinese Academy of Sciences (43.34 N, 124.12 E) (Jiang *et al* 2021). The spring maize varieties used in the field measurement were Heyu-47, Heyu-12, and Fumin-58. We measured the corn yield at 68 quadrats along the corn strips. The size of two rows \times 10 m was selected to perform yield measurements at each quadrat (Djamai *et al* 2019). During harvest, ten corn plants were selected equidistantly in each quadrat and harvested manually, and then the grain yield per plant after drying was measured. The total number of corn ears and the area in each quadrat were recorded to calculate planting density. The yield of the quadrat was calculated by the grain yield per plant and planting density.

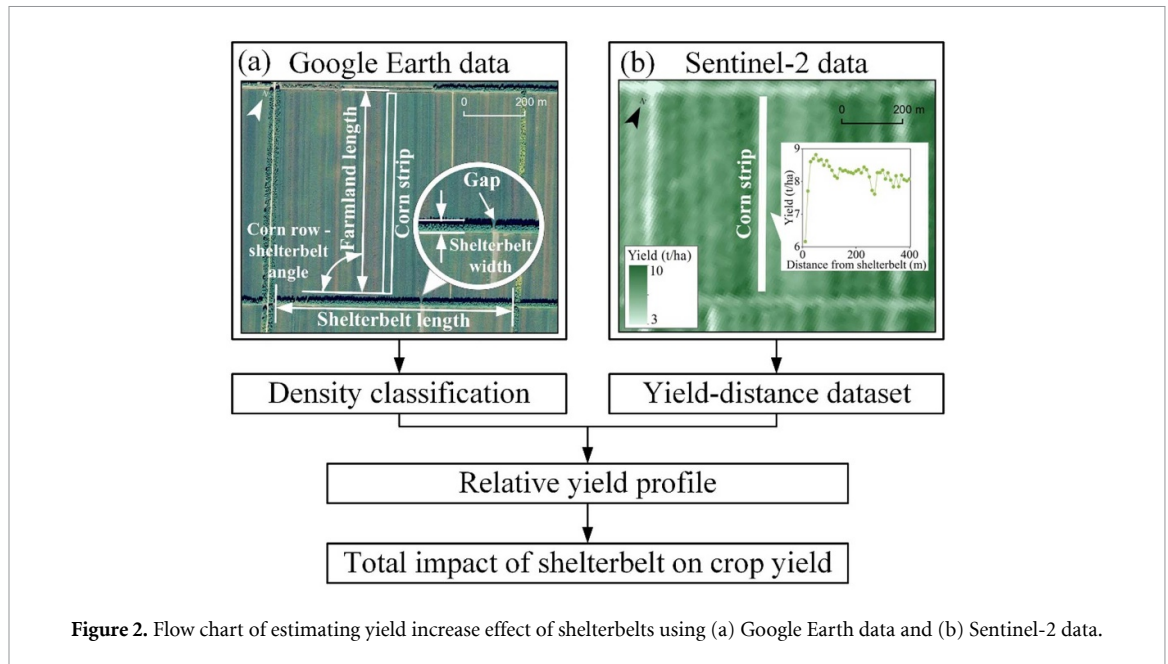


Figure 2. Flow chart of estimating yield increase effect of shelterbelts using (a) Google Earth data and (b) Sentinel-2 data.

2.3. Method

2.3.1. Selection of target shelterbelts

The target shelterbelts were selected by interpreting the historical Google Earth images in the study area from 2016 to 2019. To highlight the impact of shelterbelt structure and exclude the impact of tree height, we only selected over-mature shelterbelts, which was assumed to be 20 m (the process for determining shelterbelt height is in the supplementary files available online at stacks.iop.org/ERL/17/044060/mmedia). According to the management regulation of farm shelterbelts by the local government (Tang *et al* 2008), only over-mature shelterbelts (over 30 years) can be cut down. Thus, we checked the Google Earth images for two consecutive years for each shelterbelt. When we found the shelterbelt in the latter image was cut down, we chose the corresponding uncut shelterbelt in the previous image as the target shelterbelt. Finally, we obtained 302 target shelterbelts in total. Then we used the linear ruler tools in Google Earth Pro software to manually measure the shelterbelt length, gap length, shelterbelt width, farmland length, and corn row-shelterbelt angle (figure 2(a)).

2.3.2. Classification of shelterbelt structure

Previous studies showed that shelterbelt density was mainly affected by the width, continuity, and total area density of the shelterbelt (Deng *et al* 2013, Yang *et al* 2017, Iwasaki *et al* 2021). Total area density refers to the ratio of plant projection area to average crown length under per unit land area (Torita and Satou 2007). In the study area, the planning and planting of shelterbelts were under unified management (Zhu *et al* 2004). The difference in total area density among target shelterbelts was minor, as the tree species, tree height, and planting spacing of shelterbelts were highly similar (Zhang *et al* 2017,

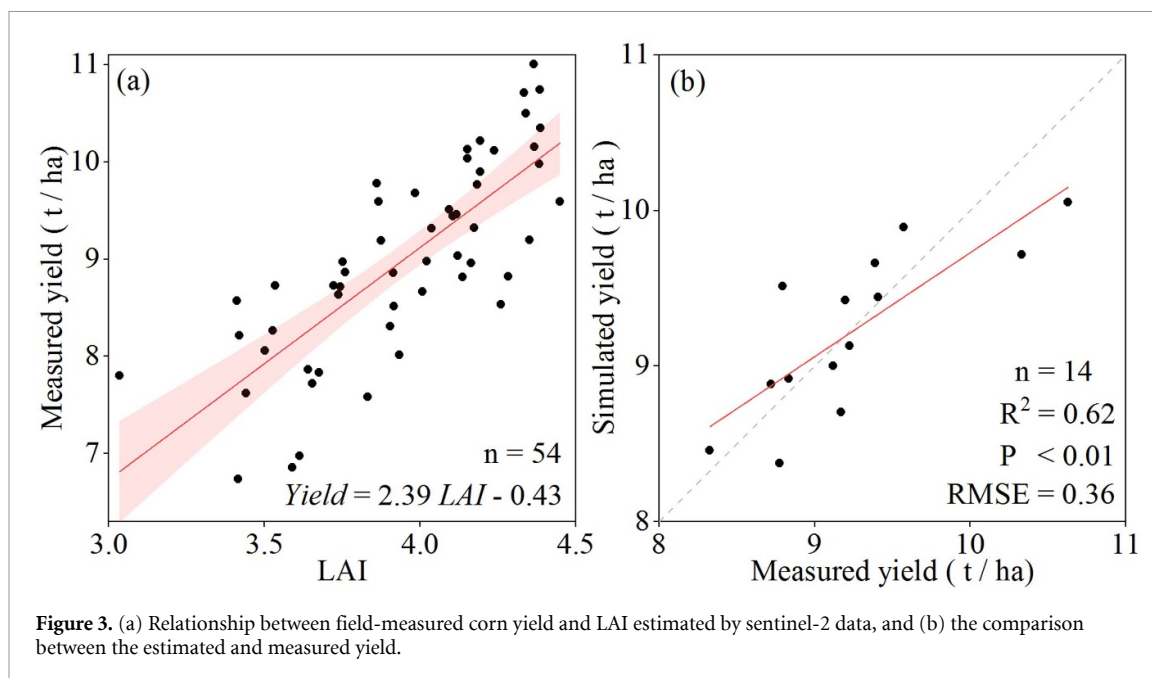
Table 1. Classification of the shelterbelt structure based on gap fraction and shelterbelt width.

Width-gap grade	Gap fraction (%)	Shelterbelt width (m)	Shelterbelt number
High	0–5	20–25	116
Medium-high	0–10	15–20	115
Medium	0–15	10–15	54
Low	0–20	5–10	17

Zhu and Zheng 2019). Moreover, the width of all target shelterbelts has no significant change before cutting down. Thus, the density of a target shelterbelt is mainly dominated by its width and continuity. Shelterbelt continuity can be expressed by gap fraction, the ratio of gap length to shelterbelt length (Piwowar *et al* 2017, Cai *et al* 2021). Combining gap fraction and shelterbelt width (figure 2(a)) (Podhrazska *et al* 2021), we defined the width-gap grade and divided it equidistantly into four different levels: high, medium-high, medium, and low (table 1). Additionally, given the influence of wind direction on the yield increase effect, we further divided the strips into leeward (north-northeast) and windward (south-southwest) groups, based on the prevailing wind direction (south-southwest) in the study area (Zhu *et al* 2003).

2.3.3. Estimation of corn yield profile

We estimated yield profiles along corn strips for the target shelterbelts. Since the farmland at the edge of shelterbelts cannot be fully protected, we only selected corn strips in the middle of target shelterbelts to estimate corn yield. All the selected corn strips met three requirements as follows: (a) the strips are uniform (only corn) and continuous (no gap); (b) the strips are along the direction of planting rows to



ensure the consistency of field management; (c) the corn row-shelterbelt angle is greater than 60° which can eliminate the influence of the shelterbelt edge.

We then calculated corn yield along the selected strips using Sentinel-2 data. Specifically, we first used the biophysical processor to convert the multi-spectral data into LAI, which is the freely available standard post-processing tool in SNAP. This processor is a collection of backpropagation artificial neural networks trained using a PROSAIL and SAILH canopy radiative transfer model (further details can be found in Weiss and Baret (2016)). The estimated LAI has high accuracy and has been validated in different regions globally (Hu et al 2020, Brown et al 2021). Here we calculated the LAI for the period of 30–60 days before harvest, which has been found to be linearly correlated with corn yield and widely used for yield estimation (Guindin-Garcia 2010, Lambert et al 2018, Endris 2019). We then developed the linear model to estimate corn yield based on the derived LAI. The parameters in the linear model were calculated based on the field measurement data (figure 3(a)). Thus, we obtained the local estimation model of corn yield (t ha^{-1}) as follows:

$$\text{Yield} = 2.39 \times \text{LAI} - 0.43. \quad (1)$$

Here, we used 80% of field measurement data to calculate the parameters in the linear model and the remaining 20% of data to verify the developed model. Generally, the developed model performed well in estimating corn yield, with $R^2 = 0.62$ and RMSE of 0.36 t ha^{-1} (figure 3(b)).

The corn yield profile was obtained based on the yield-distance relationship. Specifically, the corn yield at 10 m intervals of the Sentinel-2 images along

the strips was estimated using equation (1) (using the Bandmath processor in SNAP). The distance (D) between the shelterbelt and each yield estimation point along the corn strips was obtained based on row-oriented distance (L) and corn row-shelterbelt angle (α) and calculated as $D = L \times \sin \alpha$. Thus, we obtained the yield-distance dataset consisting of D and yield for each shelterbelt (figure 2(b)). Then we aggregated the yield-distance dataset for the four width-gap grade classifications. Based on the aggregated yield-distance dataset, we fitted the yield profile through a generalized additive model (Chen et al 2019, Baker et al 2021). Then we defined the distance at which the corn yield will not be affected by the shelterbelt as the no-impact distance, which was set as the range from 15 to 20 times the tree height (Brandle et al 2004). The average yield in the no-impact distance was set as the 100% relative yield. The yield profile was rescaled through the 100% relative yield to obtain the relative yield profile.

2.3.4. Quantification of the impact of a shelterbelt on corn yield

The impact of a shelterbelt on corn yield (i.e. yield increment) was quantified as the ratio of mean yield within the distance of 0.5–15 H to the average yield at the no-impact distance range. The data within the distance of 0–0.5 H was excluded because this area was the machine-cultivated track and rarely grew crops. We compared the impacts of shelterbelts on corn yield among the four width-gap grades classifications to reveal their relationship. In addition, the yield profiles on the leeward and windward sides with different shelterbelt width-gap grades were analyzed to compare their yield increment.

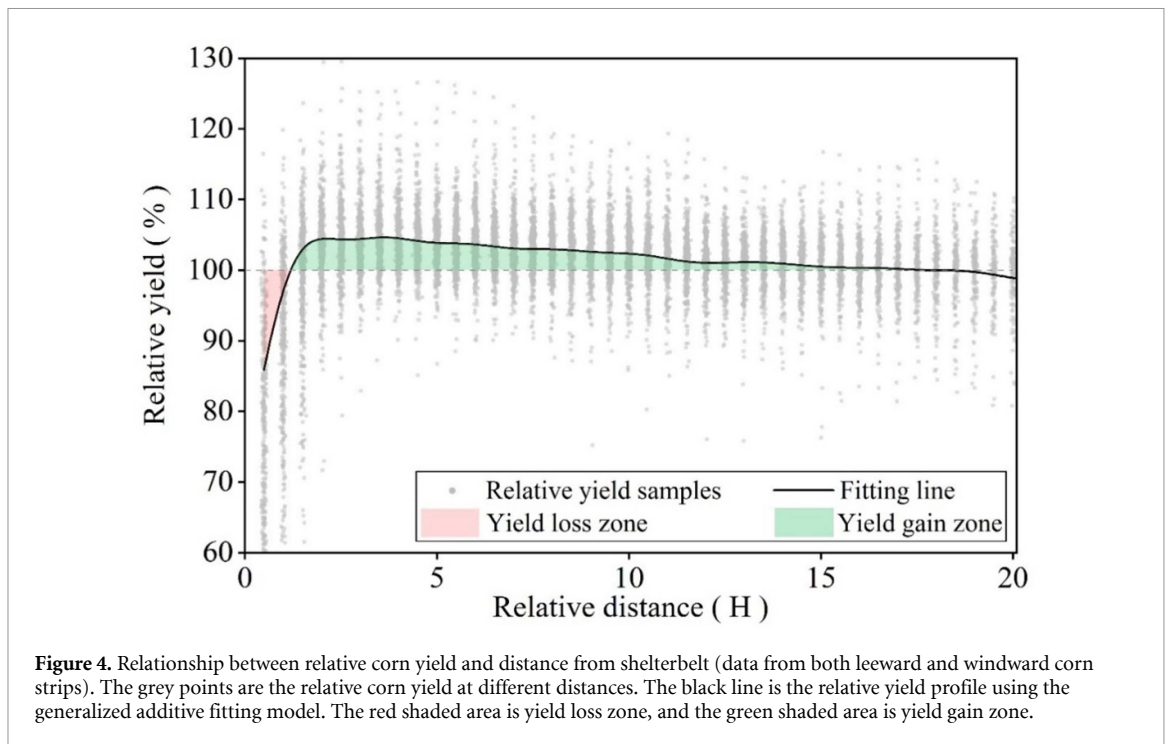


Figure 4. Relationship between relative corn yield and distance from shelterbelt (data from both leeward and windward corn strips). The grey points are the relative corn yield at different distances. The black line is the relative yield profile using the generalized additive fitting model. The red shaded area is yield loss zone, and the green shaded area is yield gain zone.

3. Results

3.1. Overall impact of shelterbelt on corn yield

The impact of a shelterbelt on the corn yield was related to the distance from the shelterbelt. Figure 4 showed the integrated yield-distance relationship of all target shelterbelts. The yield profiles consisted of both yield loss and yield gain zones. Near the shelterbelt, the corn yield was reduced due to the environmental competition between shelterbelt and corn. However, the reduced-yield effect decreased rapidly and disappeared when the distance was reaching about 1.2 H. The average reduced-yield effect was -0.32% in the yield loss zone. Beyond 1.2 H, the impact of the shelterbelt on corn yield became positive and the corn yield continuously increased, reached maximum ($4.48\% \pm 0.22\%$, mean \pm standard error, the same below) at 3.5 H and then gradually decreased till 15 H. The average increased-yield effect was 2.41% in the yield gain zone. Overall, the shelterbelts improved the corn yield by $2.09 \pm 0.04\%$. This result matched with the values (1%–6%) reported by Zheng *et al* (2016) and Nie (2020) in the study region.

3.2. Comparison of yield profiles of different shelterbelt width-gap grades

The yield profiles were largely affected by shelterbelt width-gap grade (figure 5). Both the distance range of yield loss and gain zones and the amount of yield changes varied with width-gap grades. The distance range of the yield loss zone were located within 0.5–1.2 H (high-grade), 0.5–1.2 H (medium-high-grade), 0.5–1.3 H (medium-grade) and 0.5–1.3 H (low-grade). The yield reductions of shelterbelts with

width-gap grades from high to low grade were 0.31%, 0.32%, 0.45%, and 0.47%, respectively. The lowest yield reduction happened in high-grade shelterbelts, despite the largest shading effect. This is because the yield reduction is partly offset by the protective effect caused by reduced wind, which is largest in high-grade shelterbelts (Yuan *et al* 2020). The maximum yield increase effect appeared in 2–5 H, and the corresponding amount of yield increment was in the order of high (4.70%), medium-high (4.63%), medium (4.16%), and low (3.17%) grade. Then the yield increment gradually became weak and extended beyond 15 H. In the yield gain zone, the mean yield increments were 2.32% (high-grade), 2.53% (medium-high-grade), 2.44% (medium-grade), and 1.38% (low-grade), respectively. The medium-high-grade shelterbelt had the largest yield increase effect and distance range in yield gain zone, and the smallest yield reduction effect and distance range in yield loss zone. In contrast, the low-grade shelterbelt had the opposite impact on the yield profile. Overall, medium-high-grade shelterbelts had the largest positive effect on corn yield ($2.21 \pm 0.05\%$), compared to high-grade shelterbelts ($2.01 \pm 0.06\%$), medium-grade shelterbelts ($1.99 \pm 0.11\%$), and low-grade shelterbelts ($0.91 \pm 0.12\%$). The underlying mechanism of the impact of shelterbelt width-gap grade on corn yield was discussed in section 4.

3.3. Comparison of yield profiles between windward and leeward sides

We divided all corn strips into leeward and windward groups and found that the yield profiles and their dependence on shelterbelt width-gap grade

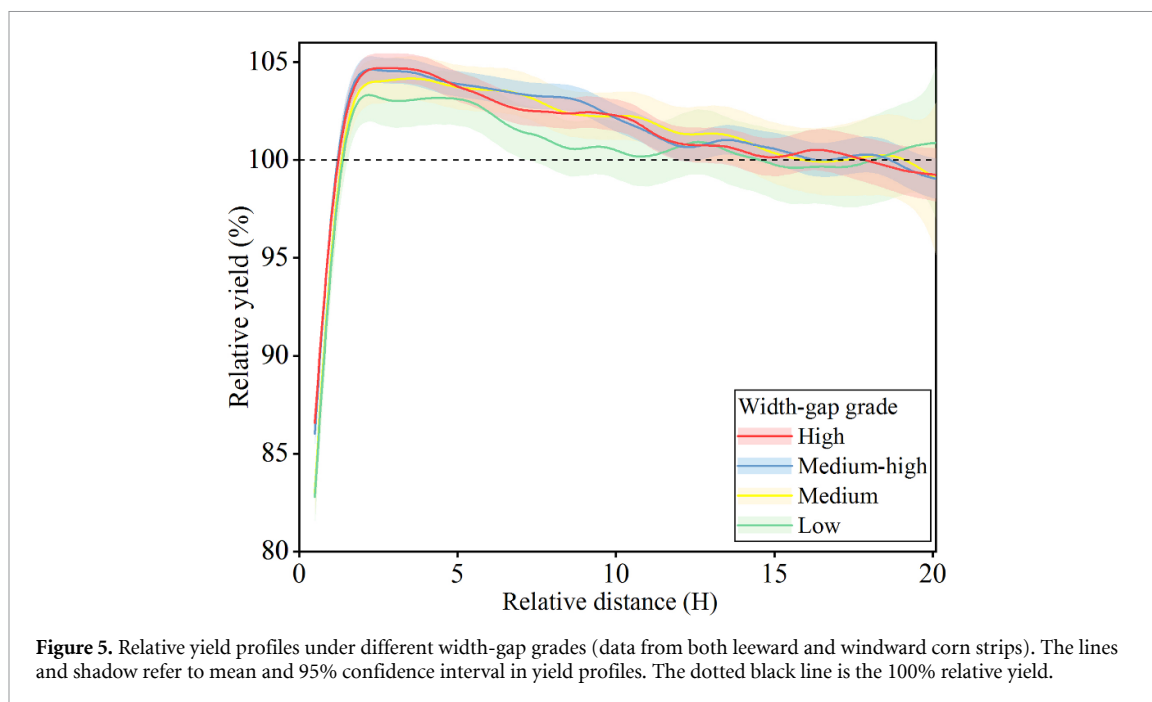


Figure 5. Relative yield profiles under different width-gap grades (data from both leeward and windward corn strips). The lines and shadow refer to mean and 95% confidence interval in yield profiles. The dotted black line is the 100% relative yield.

showed a significant difference between these two sides (figure 6). Generally, the corn on the leeward side had a larger yield increment ($2.39 \pm 0.04\%$) compared to the windward side ($1.89 \pm 0.06\%$). The distance of the yield loss zone ranged from -0.5 to $-1.5 H$ and from 0.5 to $1.1 H$ for the windward and leeward sides, respectively. The yield reduction in the yield loss zone was -0.54% on the windward side and -0.18% on the leeward side, whereas the yield increment in the yield gain zone was 2.43% on the windward side and 2.57% on the leeward side. The overall yield increments under different shelterbelt grades were in the order of medium-high ($2.17 \pm 0.07\%$), high ($1.80 \pm 0.10\%$), medium ($1.36 \pm 0.20\%$), and low ($0.67 \pm 0.13\%$) on the windward side, whereas in the order of medium-high ($2.54 \pm 0.06\%$), medium ($2.18 \pm 0.11\%$), high ($1.90 \pm 0.07\%$), and low ($1.30 \pm 0.17\%$) on the leeward side (figure 7). The protective effect of shelterbelts for leeward farmland decreased slower from medium to low grades than that for windward farmland, resulting in larger yield increments. The results of the total groups are composed of windward and leeward farmland. The protective effect of shelterbelts on the leeward side is larger than that on the windward side, leading to the higher yield increment in both the leeward and total groups. The yield reduction in the yield loss zone was -0.59% , -0.49% , -0.85% , and -0.65% for high to low grade shelterbelts on the windward side, and -0.17% , -0.19% , -0.27% , and -0.32% on the leeward side. The yield increment in the yield gain zone was 2.39% , 2.66% , 2.21% , and 1.32% for high to low grade shelterbelts on the windward side, while it was 2.07% , 2.73% , 2.45% , 1.62% on the leeward side.

4. Discussion

4.1. Impact of shelterbelt structure on corn yield

The shelterbelt impact on corn yield is a complex process and still far from being fully understood. Our results found that the yield increase effect is the addition of yield reduction in the yield loss zone and the yield increment in the yield gain zone. The total yield effect induced by a shelterbelt is positive, which is consistent with the study of Iwasaki *et al* (2021). The yield loss zone was usually caused by the competition between the shelterbelt and the corn for light, water, and nutrients (Barcic *et al* 2021, Podhrazska *et al* 2021, Thevs and Aliev 2021). In the yield gain zone of 1.2 – $15 H$, due to the wind reduction effect of the shelterbelt, the mechanical damage caused by the wind was reduced (Cleugh *et al* 1998, Cai *et al* 2021), and the microclimate was improved (Barcic *et al* 2021), therefore, corn yield increased.

The impact of a shelterbelt width-gap grade on corn yield is also complicated. Our results suggested that the increasing grade of shelterbelts cannot always bring the increasing yield increase effect, as expected initially. The largest yield increment was achieved by the shelterbelt with a medium-high width-gap grade. The shelterbelt grade was determined by shelterbelt width and gap fraction, which are closely related to wind velocity reduction (Heisler and Dewalle 1988, Yusaiyin and Tanaka 2009, Deng *et al* 2013). The wind reduction effect of shelterbelts is an important reason for the yield increase around shelterbelts (Helmert and Brandle 2005) because low wind speed means less mechanical damage, less evapotranspiration and less soil erosion (Cleugh *et al* 1998, Barcic *et al* 2021,

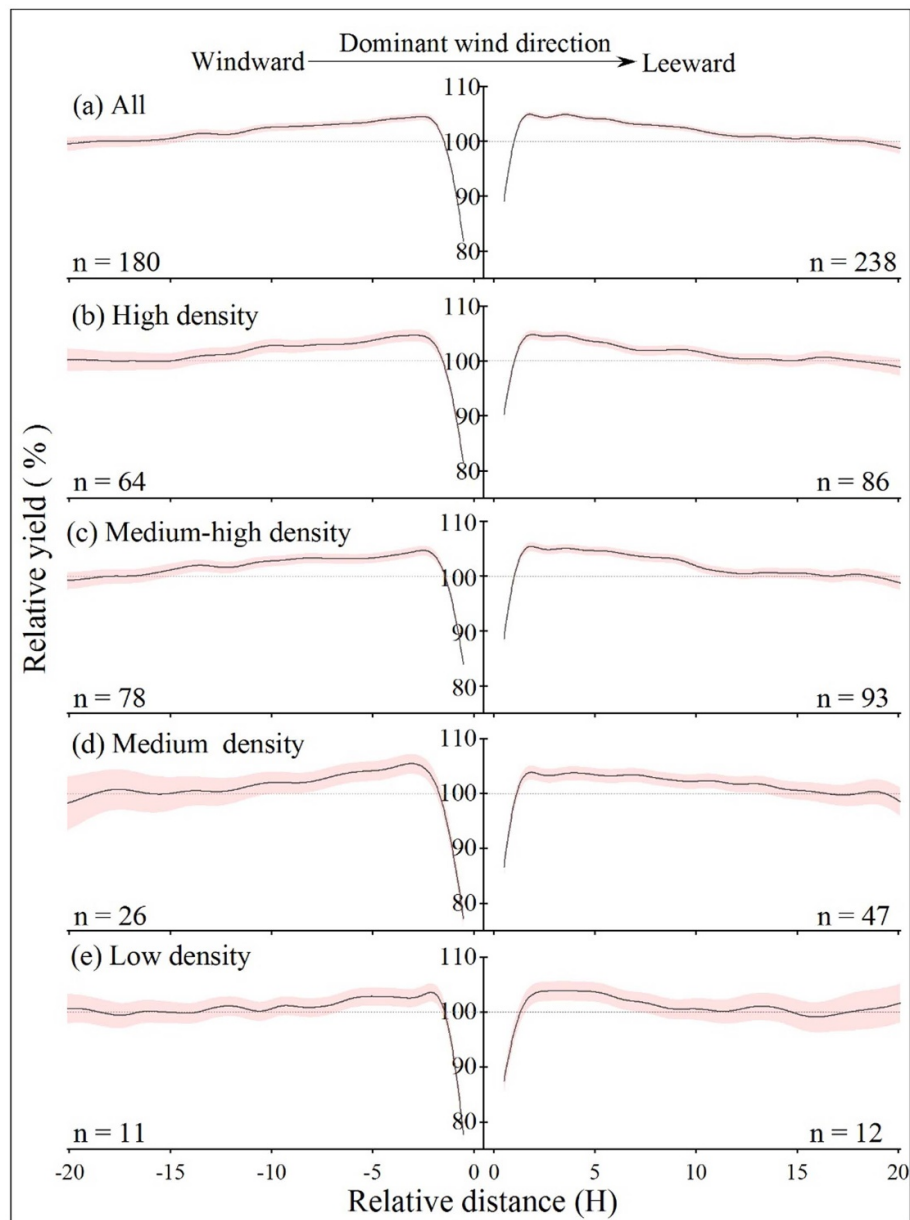


Figure 6. Comparison of relative yield profiles between windward (left) and leeward (right) sides with (a) all, (b) high, (c) medium-high, (d) medium, and (e) low width-gap grades of shelterbelts. The lines and shaded parts refer to mean yield profiles and 95% confidence interval. The n is the number of shelterbelts.

Su *et al* 2021). Dense shelterbelts have higher wind reduction near the shelterbelt. Thus, we observed that the high-grade shelterbelt had the largest yield increase effect at the range from 2 to 5 H, followed by medium-high, medium and low-grade shelterbelts (figure 5). However, the yield increase effect of a high-grade shelterbelt decreased rapidly with distance. In the range from 5 to 10 H, the maximum yield increase effect is achieved by a medium-high grade shelterbelt, followed by medium-, high- and low-grade shelterbelts. From 10 to 15 H, the maximum yield increase effect is achieved by medium-grade shelterbelts. This is because the gradient between the airflow passing through and over-passing is larger for shelterbelts with a higher grade, resulting in larger turbulence and advection transmission (Guan *et al* 2003, Li *et al* 2021,

Liu *et al* 2021). Thus, the wind speed behind a shelterbelt with higher grade recovered faster and the shelter distance was shorter. Therefore, the yield increase effect is affected by a trade-off between the distance and the amount of wind reduction.

The shelterbelt with a medium-high width-gap grade balanced the reduction in wind speed and shelter distance, resulting in the largest wind reduction effectiveness and yield increase effect. The high-grade shelterbelt had the densest structure, but the yield increment was lower than the medium-high and medium-grade shelterbelts (figure 7). The moderate grade shelterbelt produced a higher yield increment, which was consistent with the wind reduction effect (Yuan *et al* 2020). The wind reduction effect of the low-grade shelterbelt is the smallest, resulting in the

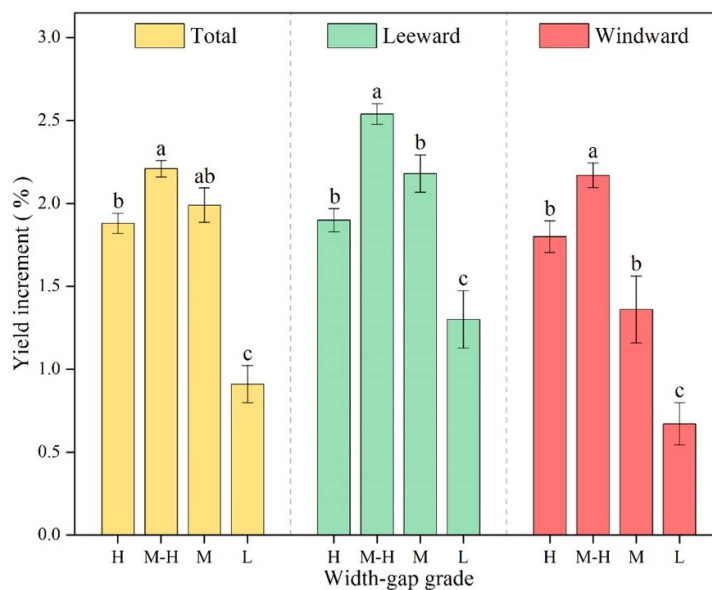


Figure 7. Comparison of yield increments under different shelterbelt groups. The column and error bar refer to yield increment mean and standard error. The yellow, green and red colors refer to total, leeward and windward groups. H: high width-gap grade, M-H: medium-high width-gap grade, M: medium width-gap grade, L: low width-gap grade. Letters (a), (b), or (c) suggest significant differences between different groups at $\alpha = 0.05$.

smallest yield increment among the four grade levels of shelterbelts (Dong *et al* 2007).

4.2. The uncertainties

The estimations of shelterbelt structure and their effect on yield increase are challenging. This new framework for obtaining the yield increase effect of a shelterbelt was developed based on several assumptions, including homogeneous shelterbelt height, shelterbelt planting spacing, corn cultivar and corn planting density. In the real world, the structure of the shelterbelt-farmland system is more complicated than the idealized assumptions. Several uncertainties may exist in this study. First, the height of all selected shelterbelts was assumed to be 20 m, which actually fluctuated in the range of 18–22 m (see supplementary file). Future studies should take into consideration the variation of shelterbelt height across species, especially in the regions with multiple species. Second, we assumed homogeneous total area density among all selected shelterbelts. However, differentiation and pest/disease are inevitable, resulting in uneven total area density of shelterbelts. We increased the sample size to reduce the uncertainty caused by this assumption. Finally, the corn cultivar and farmland planting density may also affect the impact of a shelterbelt on corn yield. Although the variation cannot be thoroughly eliminated, measures to reduce it were made in this study by selecting the corn strips along the direction of planting rows and using relative yield to describe variation. Uncertainties may also come from the process of data analysis, for example, the selection of image date and sample size of the field measurement. It is impossible to use

images from the same date in all cornfields because of cloud cover. Previous studies have shown that the LAI changes little in the time window (30–60 days before harvest), so the yield bias induced by inconsistent image date is small (Amuti *et al* 2018, Battude *et al* 2016). Furthermore, the size of field verification data used in this study was limited by field conditions. It is necessary to implement the field measurement to validate the applicability of the LAI-yield model when applying this framework to other regions.

5. Conclusions

This study developed a new framework to identify shelterbelts, and to estimate shelterbelt structure and surrounding corn yield profiles at a regional scale using high-resolution remote sensing data. Using this framework, we first quantified the impact of shelterbelt structure on corn yield. The results showed that shelterbelt forests could increase corn yield by 2.09% on average, with increments of 2.01%, 2.21%, 1.99%, and 0.91% for high, medium-high, medium, and low width-gap grade shelterbelts, respectively. These total yield increments comprised the addition of the yield loss zone (within 1.2 H) and yield gain zone (1.2–15 H). Medium-high grade shelterbelts have a well balanced relationship between wind reduction and shelter distance, resulting in the highest yield increase effect. The farmland location relative to the shelterbelt largely affected the yield increase effect, with increases of 2.39% on the leeward side and 1.89% on the windward side. Our findings are helpful in better understanding the shelterbelt impacts on crop yield and guide the practical management

of shelterbelts based on their structure, to improve crop yield. For example, thinning can be considered in a high-grade shelterbelt, to reduce shelterbelt width (Jiang *et al* 2003), whereas replanting, adding shrub borders, and enhancing the management of seedlings can be applied to medium-grade shelterbelts (Zhu and Song 2021).

Data availability statement


All data that support the findings of this study are included within the article (and any supplementary files).


Acknowledgments

This research is supported by the National Natural Science Foundation of China (Grant Nos. 31971728, 32171873) and Natural Science Foundation of Liaoning Province (Grant No. 2020-MS-027).

ORCID iDs

Yage Liu  <https://orcid.org/0000-0002-6641-2396>

Fenghui Yuan  <https://orcid.org/0000-0003-1004-873X>

Minchao Wu  <https://orcid.org/0000-0003-3557-8462>

References

- Amichev B Y, Bentham M J, Kulshreshtha S N, Laroque C P, Piwohar J M and Van Rees K C J 2017 Carbon sequestration and growth of six common tree and shrub shelterbelts in Saskatchewan, Canada *Can. J. Soil Sci.* **97** 368–81
- Amuti T, Luo G, Yin G, Hu Q and Walter-Shea E A 2018 Validation of a process-based agro-ecosystem model (Agro-IBIS) for Maize in Xinjiang, Northwest China *Agronomy* **8** 8030029
- Baker T P, Moroni M T, Hunt M A, Worledge D and Mendham D S 2021 Temporal, environmental and spatial changes in the effect of windbreaks on pasture microclimate *Agric. For. Meteorol.* **297** 10
- Baker T P, Moroni M T, Mendham D S, Smith R and Hunt M A 2018 Impacts of windbreak shelter on crop and livestock production *Crop Pasture Sci.* **69** 785–96
- Bao Y H, Li H Y and Zhao H F 2012 Effect of shelterbelts on winter wheat yields in sanded farmland of north-western Shandong province, China *J. Food Agric. Environ.* **10** 1399–403
- Barcic D, Habjanec V, Spanjol Z and Sango M 2021 Analysis of raising windbreaks on the mediterranean Karst of Croatia *Sumar. List* **145** 175–83
- Battude M, Al Bitar A, Morin D, Cros J, Huc M, Sicre C M, Le Dantec V and Demarez V 2016 Estimating maize biomass and yield over large areas using high spatial and temporal resolution Sentinel-2 like remote sensing data *Remote Sens. Environ.* **184** 668–81
- Bentrop G, Hopwood J, Adamson N L and Vaughan M 2019 Temperate agroforestry systems and insect pollinators: a review *Forests* **10** 20
- Brandle J R, Hodges L and Zhou X H 2004 Windbreaks in North American agricultural systems *New Vistas in Agroforestry: A Compendium for 1st World Congress of Agroforestry, 2004* ed P K R Nair, M R Rao and L E Buck (Dordrecht: Springer) pp 65–78
- Brown L A *et al* 2021 Validation of baseline and modified Sentinel-2 level 2 prototype processor leaf area index retrievals over the United States *ISPRS J. Photogramm. Remote Sens.* **175** 71–87
- Cai X, Henderson M, Wang L, Su Y and Liu B 2021 Shelterbelt structure and crop protection from increased typhoon activity in Northeast China *Agriculture* **11** 995
- Chen K F, O'Leary R A and Evans F H 2019 A simple and parsimonious generalised additive model for predicting wheat yield in a decision support tool *Agric. Syst.* **173** 140–50
- Cleugh H A, Miller J M and Bohm M 1998 Direct mechanical effects of wind on crops *Agrofor. Syst.* **41** 85–112
- Clevers J, Kooistra L and van den Brande M M M 2017 Using Sentinel-2 data for retrieving LAI and leaf and canopy chlorophyll content of a potato crop *Remote Sens.* **9** 15
- Deng R X, Li Y, Wang W J and Zhang S W 2013 Recognition of shelterbelt continuity using remote sensing and waveform recognition *Agrofor. Syst.* **87** 827–34
- Ding M J, Guan Q H, Li L H, Zhang H M, Liu C and Zhang L 2020 Phenology-based rice paddy mapping using multi-source satellite imagery and a fusion algorithm applied to the poyang lake plain, Southern China *Remote Sens.* **12** 18
- Ding S and Su P 2010 Effects of tree shading on maize crop within a Poplar-maize compound system in Hexi Corridor oasis, northwestern China *Agrofor. Syst.* **80** 117–29
- Djamai N, Fernandes R, Weiss M, McNairn H and Goita K 2019 Validation of the sentinel simplified level 2 product prototype processor (SL2P) for mapping cropland biophysical variables using Sentinel-2/MSI and Landsat-8/OLI data *Remote Sens. Environ.* **225** 416–30
- Dong Z B, Luo W Y, Qian G Q and Wang H T 2007 A wind tunnel simulation of the mean velocity fields behind upright porous fences *Agric. For. Meteorol.* **146** 82–93
- Drusch M *et al* 2012 Sentinel-2: ESA's optical high-resolution mission for GMES operational services *Remote Sens. Environ.* **120** 25–36
- Endris S 2019 Combined application of phosphorus fertilizer with tithonia biomass improves grain yield and agronomic phosphorus use efficiency of hybrid maize *Int. J. Agron.* **2019** 6167384
- Fang H Y 2021 Quantifying farmland shelterbelt impacts on catchment soil erosion and sediment yield for the black soil region, northeastern China *Soil Use Manage.* **37** 181–95
- Gao F, Anderson M, Daughtry C and Johnson D 2018 Assessing the Variability of Corn and Soybean Yields in Central Iowa Using High Spatiotemporal Resolution Multi-Satellite Imagery *Remote Sens.* **10** 1489
- Gochez A M, Behlau F, Singh R, Ong K, Whilby L and Jones J B 2020 Panorama of citrus canker in the United States *Tropical Plant Pathol.* **45** 192–9
- Guan D X, Zhang Y S and Zhu T Y 2003 A wind-tunnel study of windbreak drag *Agric. For. Meteorol.* **118** 75–84
- Guan D X, Zhong Y, Jin C J, Wang A Z, Wu J B, Shi T T and Zhu T Y 2009 Variation in wind speed and surface shear stress from open floor to porous parallel windbreaks: a wind tunnel study *J. Geophys. Res.* **114** 13
- Guindin-Garcia N 2010 Estimating Maize Grain Yield from Crop Biophysical Parameters Using Remote Sensing *PhD* University of Nebraska-Lincoln
- Haddaway N R, Brown C, Eales J, Eggers S, Josefsson J, Kronvang B, Randall N P and Uusi-Kamppa J 2018 The multifunctional roles of vegetated strips around and within agricultural fields *Environ. Evid.* **7** 14
- Hansen S M, Gunnell J, Whaley A, Dai X, Harding C and Black B L 2020 Adaptability of tree species as windbreaks for Urban farms in the U.S. Intermountain West *Horticulturae* **6** 9
- Heisler G M and Dewalle D R 1988 Effects of windbreak structure on wind flow *Agric. Ecosyst. Environ.* **22** 41–69
- Helmets G and Brandle J R 2005 Optimum windbreak spacing in great plains agriculture *Great Plains Res.* **27** 179–98
- Hu Q, Yang J, Xu B, Huang J, Memon M S, Yin G, Zeng Y, Zhao J and Liu K 2020 Evaluation of global decametric-resolution

- LAI, FAPAR and FVC estimates derived from Sentinel-2 imagery *Remote Sens.* **12** 12060912
- Iwasaki K, Torita H and Abe T 2020 A simple process-based model for estimating windbreak effects on soil temperature during early crop growth stage *Agrofor. Syst.* **94** 2401–15
- Iwasaki K, Torita H, Abe T, Uraike T, Touze M, Fukuchi M, Sato H, Iijima T, Imaoka K and Igawa H 2019 Spatial pattern of windbreak effects on maize growth evaluated by an unmanned aerial vehicle in Hokkaido, northern Japan *Agrofor. Syst.* **93** 1133–45
- Iwasaki K, Torita H, Touze M, Wada H and Abe T 2021 Modeling optimal windbreak design in maize fields in cool humid climates: balancing between positive and negative effects on yield *Agric. For. Meteorol.* **308** 108552
- Jiang F Q, Zhu J J, Zeng D H, Fan Z P, Du X J and Cao Y C 2003 *Management for Protective Plantations* (Beijing: China Forestry Publishing House)
- Jiang Y, Xie H and Chen Z 2021 Relationship between the amounts of surface corn stover mulch and soil mesofauna assemblage varies with the season in cultivated areas of northeastern China *Soil Tillage Res.* **213** 105091
- Kanzler M, Bohm C, Mirck J, Schmitt D and Veste M 2019 Microclimate effects on evaporation and winter wheat (*Triticum aestivum* L.) yield within a temperate agroforestry system *Agrofor. Syst.* **93** 1821–41
- Kayad A, Sozzi M, Gatto S, Marinello F and Pirotti F 2019 Monitoring within-field variability of corn yield using Sentinel-2 and machine learning techniques *Remote Sens.* **11** 20
- Kenney W A 1992 The role of salicaceae species in windbreaks *For. Chron.* **68** 209–13
- Kort J 1988 Benefits of windbreaks of windbreaks to field and forage crops *Agric. Ecosyst. Environ.* **22–23** 165–90
- Lambert M J, Traore P C S, Blaes X, Baret P and Defourny P 2018 Estimating smallholder crops production at village level from Sentinel-2 time series in Mali's cotton belt *Remote Sens. Environ.* **216** 647–57
- Li H, Claremar B, Wu L, Hallgren C, Körnich H, Ivanell S and Sahlée E 2021 A sensitivity study of the WRF model in offshore wind modeling over the Baltic Sea *Geosci. Front.* **12** 101229
- Li X Y, Liu L J, Xie J B, Wang Z Y, Yang S Y, Zhang Z Y, Qi S Z and Li Y 2020 Optimizing the quantity and spatial patterns of farmland shelter forests increases cotton productivity in arid lands *Agric. Ecosyst. Environ.* **292** 106832
- Liang J M, Gong J H and Li W H 2018 Applications and impacts of Google Earth: a decadal review (2006–2016) *ISPRS J. Photogramm. Remote Sens.* **146** 91–107
- Liu R, Zhang J J, Yang X F, Liu S M and Kang L Q 2021 Simulating airflow around flexible vegetative windbreaks *J. Geophys. Res.* **126** 19
- Nie Z 2020 Study on the Climate Effect and Crop Yield Increase Mechanism of Farmland Shelterbelt at Regional Scale MSc Shenyang Agricultural University
- Osorio R J, Barden C J and Ciampitti I A 2019 GIS approach to estimate windbreak crop yield effects in Kansas-Nebraska *Agrofor. Syst.* **93** 1567–76
- Patil R H, Hunshal C S and Itnal C J 2002 Influence of bund planted eucalyptus trees row on winter wheat *Allelopathy J.* **10** 21–28
- Piwowar J M, Amichev B Y and Van Rees K C J 2017 The Saskatchewan shelterbelt inventory *Can. J. Soil Sci.* **97** 433–8
- Podhrazska J, Kucera J, Doubrava D and Dolezal P 2021 Functions of windbreaks in the landscape ecological network and methods of their evaluation *Forests* **12** 16
- Rivest D and Vezina A 2015 Maize yield patterns on the leeward side of tree windbreaks are site-specific and depend on rainfall conditions in eastern Canada *Agrofor. Syst.* **89** 237–46
- Skakun S, Kalecinski N I, Brown M G, Johnson D M, Vermote E F, Roger J and Franch B 2021 Assessing within-Field Corn and Soybean Yield Variability from WorldView-3, Planet, Sentinel-2, and Landsat 8 Satellite Imagery *Remote Sens.* **13** 872
- Smith M M, Bentrup G, Kellerman T, MacFarland K, Straight R and Ameyaw L 2021 Windbreaks in the United States: a systematic review of producer-reported benefits, challenges, management activities and drivers of adoption *Agric. Syst.* **187** 103032
- Su Z-A, Zhou T, Zhang X-B, Wang X-Y, Wang J-J, Zhou M-H, Zhang J-H, He Z-Y and Zhang R-C 2021 A preliminary study of the impacts of shelter forest on soil erosion in cultivated land: evidence from integrated Cs-137 and Pb-210(ex) measurements *Soil Tillage Res.* **206** 104843
- Sudmeyer R A, Adams M A, Eastham J, Scott P R, Hawkins W and Rowland I C 2002 Broadacre crop yield in the lee of windbreaks in the medium and low rainfall areas of south-western Australia *Aust. J. Exp. Agric.* **42** 739–50
- Swieter A, Langhof M, Lamerre J and Greef J M 2019 Long-term yields of oilseed rape and winter wheat in a short rotation alley cropping agroforestry system *Agrofor. Syst.* **93** 1853–64
- Tamang B, Andreu M G and Rockwood D L 2010 Microclimate patterns on the leeward side of single-row tree windbreaks during different weather conditions in Florida farms: implications for improved crop production *Agrofor. Syst.* **79** 111–22
- Tang X P, Xie S X, Cui W S, Wang C H, Chen Y, Yuan S Q, Wen G Q, Zhou J M, Chen X L and Liu J J 2008 Operational regulation of harvesting of farmland shelterbelt forest vol LY/T 1723–2008 pp 1–16
- Thevs N and Aliev K 2021 Agro-economy of tree wind break systems in Kyrgyzstan, Central Asia *Agrofor. Syst.* **4** 100085
- Torita H and Satou H 2007 Relationship between shelterbelt structure and mean wind reduction *Agric. For. Meteorol.* **145** 186–94
- Weiss M and Baret F 2016 S2ToolBox level 2 products: LAI, FAPAR, FCOVER, Version 1.1 ESA Contract nr 4000110612/14/I-BG 52
- Weninger T, Scheper S, Lackóová L, Kitzler B, Gartner K, King N W, Cornelis W, Strauss P and Michel K 2021 Ecosystem services of tree windbreaks in rural landscapes—a systematic review *Environ. Res. Lett.* **16** 103002
- Wu T G, Zhang P, Zhang L, Wang J Y, Yu M K, Zhou X H and Wang G G 2018 Relationships between shelter effects and optical porosity: a meta-analysis for tree windbreaks *Agric. For. Meteorol.* **259** 75–81
- Yang X G, Yu Y and Fan W Y 2017 A method to estimate the structural parameters of windbreaks using remote sensing *Agrofor. Syst.* **91** 37–49
- Yu K J, Li D H and Li N Y 2006 The evolution of Greenways in China *Landsc. Urban Plan.* **76** 223–39
- Yuan F, Wu J, Wang A, Guan D, Zhang Y, Rajah-Boyer K I and Xu X 2020 A semiempirical model for horizontal distribution of surface wind speed leeward windbreaks *Agrofor. Syst.* **94** 499–516
- Yusaiyin M and Tanaka N 2009 Effects of windbreak width in wind direction on wind velocity reduction *J. For. Res.* **20** 199–204
- Zhang X D, Du J, Huang T, Zhang L M, Gao H, Zhao Y and Ma J M 2017 Atmospheric removal of PM2.5 by man-made three Northern Regions Shelter Forest in Northern China estimated using satellite retrieved PM2.5 concentration *Sci. Total Environ.* **593** 713–21
- Zheng X, Zhu J and Xing Z 2016 Assessment of the effects of shelterbelts on crop yields at the regional scale in Northeast China *Agric. Syst.* **143** 49–60
- Zhou X H, Brandle J R, Takle E S and Mize C W 2002 Estimation of the three-dimensional aerodynamic structure of a green ash shelterbelt *Agric. For. Meteorol.* **111** 93–108
- Zhu J J, Matsuzaki T, Lee F Q and Gonda Y 2003 Effect of gap size created by thinning on seedling emergency, survival and establishment in a coastal pine forest *For. Ecol. Manage.* **182** 339–54

- Zhu J J and Song L N 2021 A review of ecological mechanisms for management practices of protective forests *J. For. Res.* **32** 435–48
- Zhu J J and Zheng X 2019 The prospects of development of the Three-North Afforestation Program (TNAP): on the basis of the results of the 40-year construction general assessment of the TNAP *Chin. J. Ecol.* **38** 1600–10
- Zhu J Z, Zhou X C and Hu J Z 2004 Thoughts and views about the three north shelterbelt program *J. Nat. Resour.* **19** 79–85